Homogeneous cooling state of dilute granular gases of charged particles

Satoshi Takada,[1,2,a)] Dan Serero,[3] and Thorsten Pöschel[3]
[1]*Department of Physics, Kyoto University, Kitashirakawa Oiwakecho, Sakyo-ku, Kyoto 606-8502, Japan*
[2]*Yukawa Institute for Theoretical Physics, Kyoto University, Kitashirakawa Oiwakecho, Sakyo-ku, Kyoto 606-8502, Japan*
[3]*Lehrstuhl für Multiscale Simulation, Friedrich-Alexander-Universität Erlangen-Nürnberg, Nägelsbachstr. 49b, 91052 Erlangen, Germany*

(Received 20 December 2016; accepted 1 August 2017; published online 21 August 2017)

We describe the velocity distribution function of a granular gas of electrically charged particles by means of a Sonine polynomial expansion and study the decay of its granular temperature. We find a dependence of the first non-trivial Sonine coefficient, a_2, on time through the value of temperature. In particular, we find a sudden drop of a_2 when temperature approaches a characteristic value, T^*, describing the electrostatic interaction. For lower values of T, the velocity distribution function becomes Maxwellian. The theoretical calculations agree well with numerical direct simulation Monte Carlo to validate our theory. *Published by AIP Publishing.* [http://dx.doi.org/10.1063/1.4993620]

I. INTRODUCTION

Granular materials, i.e., collection of macroscopic grains, with dissipative interactions are commonplace in nature and industry. From rock and snow avalanches, mud slides and debris flows up to planetary rings, examples of naturally occurring granular flows are numerous. In addition, handling, conveying, and storing of grains are of great industrial importance. In most cases, agitated dry grains are electrically charged due to contact electrification, typically during transport. This feature is of great importance for industrial applications.[1–6] So far, however, the effect of electric charge on the dynamical behaviour of granular flows has hardly been addressed. When sufficiently fluidized, the interparticle interactions are dominated by binary, nearly instantaneous collisions, characterizing a flow regime referred to as a granular gas. In spite of the obvious analogy to the classical picture of molecular gases, a critical difference is the fact that in each collision, the energy is irreversibly transferred to the internal degrees of freedom of the grains. This process is characterized by the coefficient of restitution, e, defined as the ratio between the normal components of the precollisional and postcollisional relative velocities of the colliding grains. A basic consequence of the inelasticity of the collisions is the fact that in the absence of external forces, the kinetic energy of homogeneous granular gases continuously decays in time. In the case of constant coefficients of restitution, this decay is described by Haff's law,[7] which predicts that the energy decays in time as t^{-2}. The dissipative nature of particle interaction implies that granular gases are *always* in non-equilibrium, which gives rise to many interesting phenomena, such as non-Maxwellian velocity distribution[8] or the instability of the homogeneous state in the long-time evolution[9] which may be transient, depending on the details of the particle interaction.[10] In that respect, a major difference exists between the collisional behaviours of charged and uncharged granular particles. A collision between neutral hard sphere particles happens when the impact parameter is less than the sum of the particle radii. If the particles carry charges, an energy barrier induced by the electrical charges has to be overcome in order for a dissipative collision to happen. Scheffler and Wolf[11] have considered this process and derived the evolution of the kinetic energy of charged granular gases. They have found that, in contrast to Haff's law, the decay of the granular temperature is proportional to the inverse logarithm of time. Interestingly, this behavior is similar to that predicted by a simple model of viscoelastic granular gases, where the dependence of the restitution coefficient on the relative speed[12] is represented by a step function, describing collisions with a constant coefficient of restitution above a certain velocity threshold and elastic collisions below. In both situations, however, a Maxwellian form for the velocity distribution function (VDF)[11,12] has been assumed. As mentioned, it is however well known that the distribution function of granular gases may present significant deviations from the Maxwellian distribution as a consequence of the inelasticity of the collisions.[13]

In this paper, we investigate the homogeneous cooling state of charged granular gases. In particular, we derive the deviation of the velocity distribution function from the Maxwellian distribution and the evolution of the granular temperature. The charges of the grains are taken into account via a velocity dependent coefficient of restitution which captures the effects of a repulsive interaction potential associated with inelastic hard sphere collisions: The coefficient of restitution varies continuously from an elastic value at low impact velocity to a constant inelastic value for large collisional velocity, representing the fact that the energy barrier induced by the electrical charges translates into the existence of an impact velocity threshold to be reached for an inelastic hard sphere collision to occur.

[a)]Present address: Earthquake Research Institute, The University of Tokyo, 1-1-1 Yayoi, Bunkyo-ku, Tokyo 113-0032, Japan. Electronic mail: takada@eri.u-tokyo.ac.jp.

In general, systems of charged macroscopic particles reveal a variety of phenomena mainly determined by the relations between charge, Q, mass, m, particle size, σ, particle number density, n, and temperature, T. The subject of the current manuscript, namely the regime of homogeneous gases described on the level of the Boltzmann equation, restricts, of course, the range of admissible parameters. *Inelasticity* implies that the particles can come into mechanical contact at typical velocity corresponding to the given temperature (which may change in the course of its evolution). This means that the forces should be dominated by inertia not charge, restricting $Q^2/(Td) \ll 1$ (where m enters through T) to small values. The application of the Boltzmann equation implies that for a certain collision between two particles, other particles can be neglected. In the case of uncharged system, the description can be extended to moderately dense systems by employing the equilibrium pair correlation function at contact to account for spatial correlations between the particles, yielding the Enskog equation. In the case of charged grains, an analytical expression for the pair correlation function is lacking and we therefore restrict the present analysis to small values of the volume fraction. From these arguments, we conclude that the present theory is restricted to homogeneous gases of low particle number density and small values of charge carried by the particles.

The organization of this paper is as follows: In Sec. II, we introduce our model and in Sec. III we derive the expression of the coefficient a_2, which characterizes the deviation of the VDF from the Maxwellian. Section IV presents the results obtained from Direct Simulation Monte Carlo (DSMC) that we perform to check the validity of the analytical results, and we summarize our results in Sec. V. In Appendix A, we present the calculation of the second and fourth moments of the Boltzmann collision operator, by exploiting a generic integral, the Basic Integral, that we defined and evaluate. In Appendix B, the moments are derived in the limit of discontinuous restitution coefficient.

II. MODEL DESCRIPTION

We consider a monodisperse collection of spherical particles whose mass and diameter are m and σ, respectively. The particles collide inelastically yielding the following relations between the pre-collisional velocities $(\boldsymbol{v}_1, \boldsymbol{v}_2)$ and the post-collisional velocities $(\boldsymbol{v}_1', \boldsymbol{v}_2')$:

$$\begin{cases} \boldsymbol{v}_1' = \boldsymbol{v}_1 - \dfrac{1+e(\boldsymbol{v}_{12}\cdot\hat{\boldsymbol{k}})}{2}(\boldsymbol{v}_{12}\cdot\hat{\boldsymbol{k}})\hat{\boldsymbol{k}} \\ \boldsymbol{v}_2' = \boldsymbol{v}_2 + \dfrac{1+e(\boldsymbol{v}_{12}\cdot\hat{\boldsymbol{k}})}{2}(\boldsymbol{v}_{12}\cdot\hat{\boldsymbol{k}})\hat{\boldsymbol{k}} \end{cases}, \tag{1}$$

where e is the coefficient of restitution. The effect of the charge is taken into account through the velocity dependence of the coefficient of restitution which is assumed to be described by the following sigmoid like form:

$$e(v_n) = \frac{e^* \exp\left[\beta(v_n - v^*)\right] + 1}{\exp\left[\beta(v_n - v^*)\right] + 1}, \tag{2}$$

(see Fig. 1) where v_n is the normal component of the relative velocity, v^* is a characteristic velocity, β characterizes the width of the velocity range corresponding to the transition between elastic and inelastic collisions around $v = v^*$,

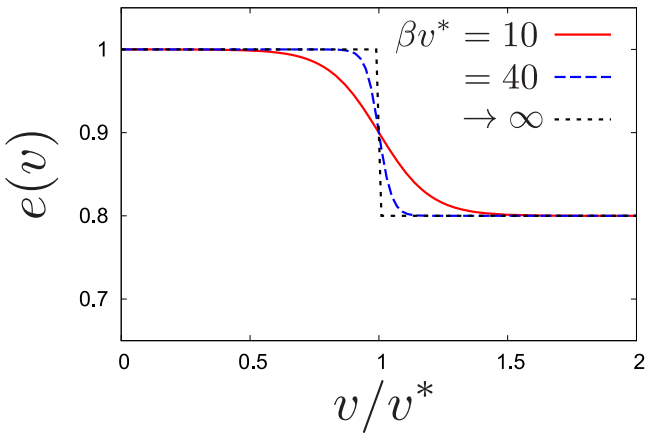

FIG. 1. Velocity dependence of the restitution coefficient e for $\beta v^* = 10$ (red solid line) 40 (blue dashed line), and $\beta v^* \to \infty$ (black dotted line).

and e^* is the (constant) restitution coefficient describing the inelastic collisions. Notice that for $\beta v^* \to \infty$, Eq. (2) reduces to $e(v_n) = 1 - \Theta(v_n - v^*)(1 - e^*)$, where $\Theta(x)$ is a step function, which is used in Ref. 12.

III. HOMOGENEOUS COOLING STATE

The Homogeneous Cooling State (HCS) of a granular gas designates a force free, homogeneous and isotropic gas in which the absolute velocity of the particles continuously decays in time, due to the inelasticity of the collisions. This state corresponds to the early stages of the evolution of an initially uniform free granular gas and has been employed in the derivation of Green-Kubo relations for granular gases,[14,15] as well as in the Chapman-Enskog perturbative scheme (as a zeroth order) to obtain transport coefficients (see, e.g., Ref. 16). The velocity distribution function (VDF) $f(v)$ is (except for large velocities[17]) a distorted Maxwellian characterized by a scaling behaviour where the time dependence occurs exclusively through the granular temperature, T, defined by its second moment as

$$\frac{3}{2}nT \equiv \int d\boldsymbol{v}\frac{m}{2}v^2 f(v). \tag{3}$$

This evolution of the granular temperature can be obtained by considering the corresponding moment of the Boltzmann equation pertaining to a granular gas (see, e.g., Refs. 13 and 18) as

$$\frac{dT}{dt} = -\frac{2}{3}n\sigma^2 g_2\sqrt{\frac{2T}{m}}\mu_2 T, \tag{4}$$

where n is the number density field, σ is the diameter of particles, g_2 is the radial distribution function at contact which is in the sequel set to one as we consider dilute systems, and μ_2 is the second moment of the dimensionless collision integral, whose general definition is given by

$$\mu_p = -\frac{1}{2}\int d\boldsymbol{c}_1 \int d\boldsymbol{c}_2 \int d\hat{\boldsymbol{k}} \times \Theta(-\boldsymbol{c}_{12}\cdot\hat{\boldsymbol{k}})|\boldsymbol{c}_{12}\cdot\hat{\boldsymbol{k}}|\tilde{f}(\boldsymbol{c}_1)\tilde{f}(\boldsymbol{c}_2)\Delta[c_1^p + c_2^p], \tag{5}$$

with $\Delta\psi(\boldsymbol{c}_i) \equiv \psi(\boldsymbol{c}_i') - \psi(\boldsymbol{c}_i)$ designating the change in the collision of the velocity dependant quantity ψ, where $\boldsymbol{c}_i \equiv \boldsymbol{v}_i/v_{\mathrm{T}}$ is the nondimensional velocity with the thermal velocity

$v_T = (2T/m)^{1/2}$, and $\boldsymbol{c}_{ij} = \boldsymbol{c}_i - \boldsymbol{c}_j$. As mentioned, in the HCS, the VDF is (essentially) near Maxwellian. The deviation from Maxwell's distribution may be described by a correction in the form of an expansion in Sonine polynomials. We consider here the first non-trivial truncation of the expansion so that the dimensionless distribution function $\tilde{f}(c)$ is given by

$$\tilde{f}(c) = \phi(c)\left[1 + a_2 S_2^{(1/2)}(c^2)\right], \tag{6}$$

where $\phi = \pi^{-3/2}\exp(-c^2)$ is the dimensionless Maxwell distribution function and $S_p^{(m)}(x)$ are the Sonine polynomials defined by

$$S_p^{(m)}(x) = \sum_{n=0}^{p} \frac{(-1)^n (m+p)!}{(m+n)!(p-n)!n!} x^n. \tag{7}$$

The dimensionless dissipation rate μ_2 is given by

$$\begin{aligned}\mu_2 =& -\frac{1}{2}\int d\boldsymbol{c}_1 \int d\boldsymbol{c}_2 \int d\hat{\boldsymbol{k}} \\ &\times \Theta(-\boldsymbol{c}_{12}\cdot\hat{\boldsymbol{k}})|\boldsymbol{c}_{12}\cdot\hat{\boldsymbol{k}}|\tilde{f}(\boldsymbol{c}_1)\tilde{f}(\boldsymbol{c}_2)\Delta[c_1^2 + c_2^2] \\ \equiv& \sqrt{2\pi}(S_1 + a_2 S_2),\end{aligned} \tag{8}$$

where S_1 and S_2 are given by Eqs. (A6) and (A7), respectively (the detailed derivation is given in Appendix A). Similarly, the fourth moment μ_4 can be calculated as

$$\begin{aligned}\mu_4 =& -\frac{1}{2}\int_0 d\boldsymbol{c}_1 \int d\boldsymbol{c}_2 \int d\hat{\boldsymbol{k}} \\ &\times \Theta(-\boldsymbol{c}_{12}\cdot\hat{\boldsymbol{k}})|\boldsymbol{c}_{12}\cdot\hat{\boldsymbol{k}}|\tilde{f}(\boldsymbol{c}_1)\tilde{f}(\boldsymbol{c}_2)\Delta[c_1^4 + c_2^4] \\ \equiv& \sqrt{2\pi}(T_1 + a_2 T_2),\end{aligned} \tag{9}$$

where T_1 and T_2 are given by Eqs. (A9) and (A10), respectively. From the properties of the collision integral and the moment of the velocities,[13] that is, $5\mu_2(1+a_2) = \mu_4$, we can determine the coefficient a_2 as

$$a_2 = \frac{T_1 - 5S_1}{5S_1 + 5S_2 - T_2}, \tag{10}$$

under the linear approximation with respect to a_2, expected to be valid when the particles are not strongly inelastic. Figure 2 shows the temperature dependence of the coefficient a_2 for various values of βv^*. Here, T^* is the characteristic temperature defined by the characteristic velocity v^* as $T^* = mv^{*2}/2$. In this figure, we also compare with the result for the discontinuous ($\beta v^* \to \infty$) limit of a_2, whose explicit form is given in Appendix B. In the high (low) temperature limit, the coefficient a_2 converges to that of hard-core gases (0), from the fact that almost all particles collide inelastically (elastically) at this temperature as shown in Fig. 1. However, noticeably, the coefficient a_2 exhibits a minimum at intermediate temperature. This peak also appears in the previous studies[13,19] although the velocity dependence of the restitution coefficient is different from that of the present results. Figure 3 shows the temperature dependence of a_2 for various restitution coefficients e^*. Here, $a_{2,\mathrm{HC}}$ is the one for hard-core gases, whose dependence is given by $a_{2,\mathrm{HC}} = 16(1-e^*)(1-2e^{*2})/(81 - 17e^* + 30e^*(1-e^{*2}))$.[13] For each e^*, the peak appears around $T \sim 0.3T^*$.

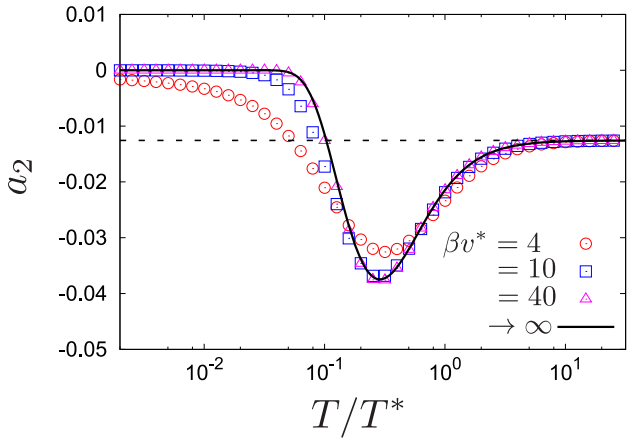

FIG. 2. Temperature dependence of a_2 for $\beta v^* = 4$ (red open circles), 10 (blue open squares), and 40 (pink open triangles). Here, we fix the value $e^* = 0.8$. The solid line is that of the discontinuous model for $e^* = 0.8$ and the dashed line is that of hard-core for $e = 0.8$.

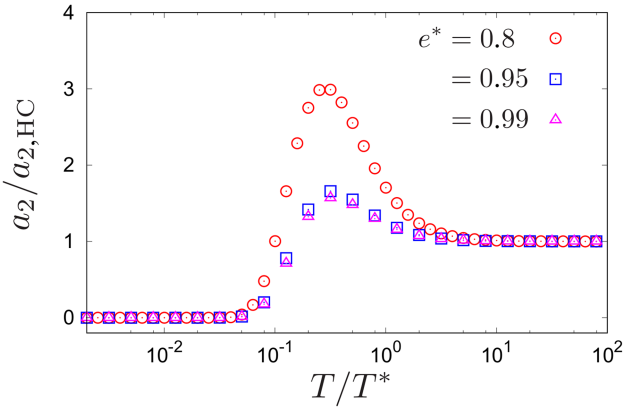

FIG. 3. Temperature dependence of a_2 for $e^* = 0.8$ (red open circles), 0.95 (blue open squares), and 0.99 (pink open triangles). Here, we fix the value $\beta v^* = 40$.

Consider next the evolution of the temperature. Figure 4 shows the evolution of the temperature. In the initial stage, the evolution obeys Haff's law for the hard-core particles.[7] This is because almost all collisions are inelastic as shown

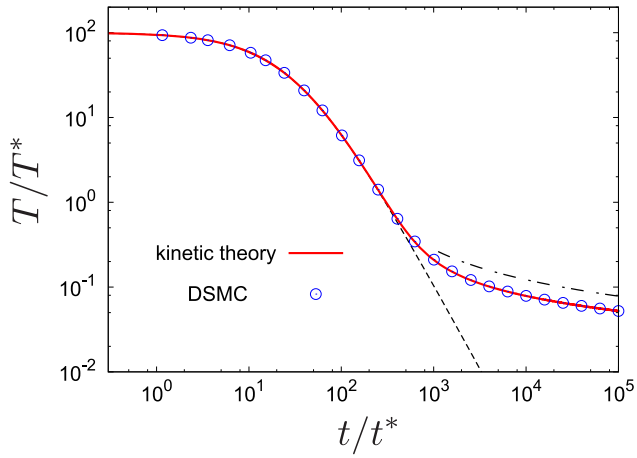

FIG. 4. Evolution of the temperature obtained from the kinetic theory (red solid line) and from the DSMC (blue open circles) for $e^* = 0.8$ and $\beta v^* = 40$, where $t^* = d/v^*$. Here, the initial temperature is $10^2\, T^*$. The dashed curve is Haff's law for $e = 0.8$ and the dot dashed line is the evolution in the later stage of viscoelastic particles given by Eq. (12), where the Maxwell distribution and the discontinuous restitution coefficient are assumed.

in Fig. 1. As time goes on, the temperature decreases, and the ratio of elastic collisions increases, which means that the decay of the temperature becomes slower than that for the hard-core. This asymptotic behaviour was analytically obtained for a system characterized by a restitution coefficient given by $e(v_n) = 1 - \Theta(v_n - v^*)(1 - e^*)$, assuming Maxwellian velocity distribution.[12] After some manipulation, we can write the evolution of the temperature as

$$\dot{x} = \alpha \left(x^{3/2} + x^{1/2} \right) e^{-x}, \tag{11}$$

where we have introduced the variable $x = mv^{*2}/(4T(t)) = T^*/(2T(t))$ and the coefficient $\alpha = (4/3)\sqrt{\pi T^*/(2m)}(1 - e^{*2})n\sigma^2$. Notice that our choice of x is the inverse of that in Ref. 12. At the later stage of the temperature evolution ($t \to \infty$), the variable x becomes sufficiently large, which leads the following asymptotic solution:[12]

$$T(t) = \frac{mv^{*2}}{4} \frac{1}{\log \alpha t} = \frac{T^*}{2} \frac{1}{\log \alpha t}. \tag{12}$$

Figure 4 shows that Eq. (12) reproduces the later stage of the temperature evolution qualitatively. Notice that there appears small discrepancy between the result of the kinetic theory and Eq. (12). This might come from the fact that the temperature in the later stage is not sufficiently large in our system. Indeed, the temperature is about $10^{-1}T^*$, i.e., $x \sim 5$ in the later stage in our system as in Fig. 4.

IV. DSMC

In order to understand the existence of the negative peak of a_2, we have performed DSMC simulations[20–25] of a monodisperse system consisting of 10^7 particles. By definition, a granular gas in the homogeneous cooling state is infinitely spread and stays homogeneous in the course of time. The evolution of a granular gas is, thus, determined by the evolution of the particles' velocities only. Therefore, the spatial coordinate of the particles is unimportant and can be disregarded in the simulation. Consequently, the system size and boundary conditions are no relevant parameters for the DSMC simulation and need, thus, not to be specified. Since DSMC is a practical and accurate method to integrate the Boltzmann equation, it is ideally suited to check the correctness of the calculations and the validity of the approximations employed in the course of the analytical calculations.

Figure 4 presents the evolution of the temperature resulting from the DSMC simulations together with that calculated from the kinetic theory employing the same parameters and shows a good agreement. We show the deviation of the VDF measured from the DSMC from the Maxwell distribution function for various temperature in Fig. 5, where $v_T = (2T/m)^{1/2}$ is the thermal velocity. First, in the low temperature regime, the deviation is small, which means that the VDF is well reproduced by the Maxwell distribution function. This is consistent with the fact that the almost all of the collisions are elastic in this regime. Next, in the high temperature regime, there exists a deviation, which is, however, well reproduced by $a_{2,\mathrm{HC}}S_2(c^2)$ as shown in Fig. 5 with $a_{2,\mathrm{HC}}$ for inelastic hard-core gases. This is because inelastic collisions are dominant. Let us focus on the intermediate temperature regime. In this

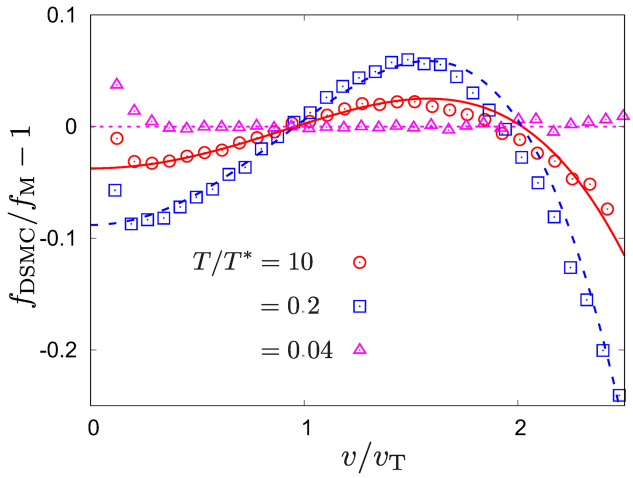

FIG. 5. The deviation of the VDF measured from the DSMC from the Maxwell distribution function for $T/T^* = 10$ (red open circles), 0.2 (blue open squares), and 0.04 (pink open triangles), where $\beta v^* = 40$ and $e^* = 0.8$. Here, $v_T = (2T/m)^{1/2}$ and f_M are the thermal velocity and the Maxwell distribution function, respectively. Each lines represents $a_2 S_2^{(1/2)}(c^2)$ and the dimensionless velocity $c \equiv v/v_T$ for each corresponding temperature. For small velocity, $v/v_T \to 0$, the numerical data reveal large fluctuations corresponding to the small frequency of finding particles at such small velocity due to the distribution $f \sim \exp\left[-(v - v_T)^2\right]$.

regime, the deviation becomes larger than that in the high temperature regime, however, even in this regime, the deviation can be fitted by $a_2 S_2(c^2)$. The large deviation agrees with the fact that a_2 has a negative peak for $T \sim 0.3\,T^*$ as shown in Fig. 2. We can understand this as follows: Let us consider the evolution of the system. In this intermediate temperature regime, particles having high velocities collide inelastically and those having low velocities collide elastically. The former lose their velocities and the population decreases as time goes on, while the latter keeps their population. After all, the number of particles having the velocity around v^* is relatively larger than that having other velocity. This is consistent with the fact that $v \sim v^*$ for $T \sim 0.2T^*$ corresponds to $v/v_T \sim 2$ in Fig. 5.

In order to further analyze the existence of the minimum of a_2, consider next an effective restitution coefficient of restitution e_{eff}, defined by the relation

$$1 - e_{\mathrm{eff}}^2 = (1 - e^{*2})(1 + x)e^{-x}, \tag{13}$$

where the right-hand side of Eq. (13) is equivalent to S_1 for $\beta v^* \to \infty$ as shown in Appendix B. We also define a_2 for hard-core gases with this effective restitution coefficient e_{eff} as $a_{2,\mathrm{eff}} = 16(1 - e_{\mathrm{eff}})(1 - 2e_{\mathrm{eff}}^2)/(81 - 17e_{\mathrm{eff}} + 30e_{\mathrm{eff}}^2(1 - e_{\mathrm{eff}}))$. The derivative of $a_{2,\mathrm{eff}}$ with respect to the temperature T becomes

$$\frac{da_{2,\mathrm{eff}}}{dT} = \frac{512(1 - e^{*2})(1 + 6e^* - 10e^{*2} + 2e^{*3})}{(81 - 17e_{\mathrm{eff}} + 30e_{\mathrm{eff}}^2(1 - e_{\mathrm{eff}}))^2 e_{\mathrm{eff}} T} x^2 e^{-x}, \tag{14}$$

which shows that $a_{2,\mathrm{eff}}$ becomes a minimum at $e_{\mathrm{eff,min}} = 0.8653$ in the range $0 < e_{\mathrm{eff}} < 1$. From Eq. (13), the corresponding temperature can be determined by

$$(1 + x)e^{-x} = \frac{0.2512}{1 - e^{*2}}. \tag{15}$$

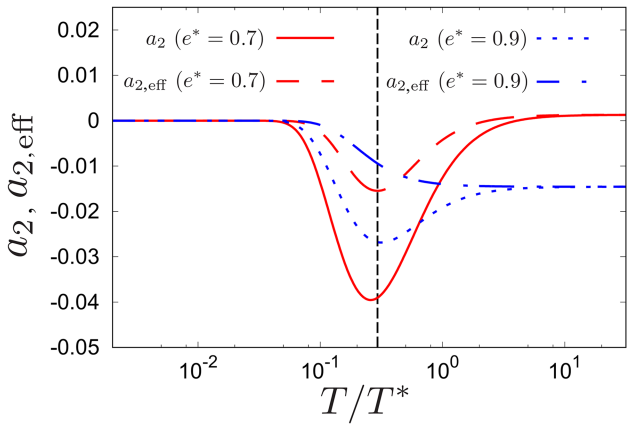

FIG. 6. The comparison between a_2 for $e^* = 0.7$ (red solid line) and 0.9 (red dashed line) determined from Eq. (10) and $a_{2,\mathrm{eff}}$ for $e^* = 0.7$ (blue dotted line) and 0.9 (blue dot dashed line). The vertical black dashed line is $T_{\min} = 0.2938T^*$, which is the solution of Eq. (15) for $e^* = 0.7$.

For $e^* = 0.7$, the solution is $T_{\min} = 0.2938T^*$. Figure 6 shows the comparison between a_2 for $\beta v^* \to \infty$ and $a_{2,\mathrm{eff}}$. The peak position of $a_{2,\mathrm{eff}}$ determined from Eq. (15) is in good agreement with that of a_2, though the peak value shows less quantitative agreement. It is also noted that Eq. (15) has no solution for $e^* > e_{\mathrm{eff,\,min}}$ because the right hand side of Eq. (15) becomes larger than unity while the left-hand side is less than unity. In this case, $a_{2,\mathrm{eff}}$ has no extreme value as shown in Fig. 6.

V. CONCLUSION

In this paper, we have employed kinetic theory to evaluate the deviation of the velocity distribution function corresponding to the homogeneous cooling state of granular gases of charged particles from the Maxwellian distribution. Among the finding, we have shown that the first non-trivial Sonine polynomial expansion coefficient exhibits a minimum at a finite value of the temperature. We have also obtained the evolution of the temperature, which obeys Haff's law in the initial stage, while the decay becomes slower in the later stage. The theoretical results were found in very good agreement with the results of DSMC simulations. We have also showed that the peak position of a_2 could be reproduced by the standard hard-core expression for the second Sonine coefficient if one considers an effective restitution coefficient correctly describing the cooling behavior of the gas at a given temperature.

ACKNOWLEDGMENTS

We acknowledge funding by Deutsche Forschungsgemeinschaft through the Cluster of Excellence "Engineering of Advanced Materials," ZISC and FPS. One of the authors (S.T.) wishes to express his sincere gratitude to the Yukawa Institute for Theoretical Physics for financial support for his stay in Friedrich-Alexander-Universität Erlangen-Nürnberg. Numerical computation in this work was partially carried out at the Yukawa Institute Computer Facility.

APPENDIX A: BASIC INTEGRAL AND THE MOMENTS OF THE COLLISION INTEGRAL

In this appendix, let us calculate the second and fourth moments of the dimensionless collision integral. First, we define the Basic Integral[13] as

$$\begin{aligned} J_{k,l,m,n,p,\alpha}\left[f(e)\right] &\equiv \int d\boldsymbol{C}\int d\boldsymbol{c}_{12}\int d\hat{\boldsymbol{k}} f(e)\Theta(-\boldsymbol{c}_{12}\cdot\hat{\boldsymbol{k}})|\boldsymbol{c}_{12}\cdot\hat{\boldsymbol{k}}|^{1+\alpha}\phi(C)\phi(c_{12})C^k c_{12}^l(\boldsymbol{C}\cdot\boldsymbol{c}_{12})^m\left(\boldsymbol{C}\cdot\hat{\boldsymbol{k}}\right)^n(\boldsymbol{c}_{12}\cdot\hat{\boldsymbol{k}})^p \\ &= \frac{(-1)^{n+p}}{\sqrt{\pi}}2^{-(k+m+n+1)/2}\frac{\Gamma\left(\frac{k+m+n+3}{2}\right)}{\Gamma\left(\frac{m+n+3}{2}\right)}\sum_{j=0}^{n}\binom{n}{j}\left[1+(-1)^j\right]\left[1+(-1)^{m+n}\right]\Gamma\left(\frac{j+1}{2}\right)\Gamma\left(\frac{m+n-j+1}{2}\right) \\ &\quad\times\int_0^\infty dc_{12}\int_0^1 d(\cos\theta)f[e(c_{12}\cos\theta)](1-\cos^2\theta)^{j/2}\cos^{n+p+\alpha-j+1}\theta c_{12}^{l+m+p+\alpha+3}\exp\left(-\frac{1}{2}c_{12}^2\right). \end{aligned} \tag{A1}$$

It is noted that this Basic Integral is the modification of that for hard-core gas given in Ref. 13. We also note that this integral becomes a functional because the restitution coefficient is a function of c_{12} and θ as $e = e(c_{12}\cos\theta)$. For three-dimensional system for the cases of $n = 0$, 1, and 2, Eq. (A1) reduces to

$$\begin{aligned} J_{k,l,m,0,p,\alpha}\left[f(e)\right] &= \frac{(-1)^p\cdot 2^{-(k+m-3)/2}}{m+1}\left[1+(-1)^m\right]\Gamma\left(\frac{k+m+3}{2}\right) \\ &\quad\times\int_0^\infty dc_{12}\int_0^1 d(\cos\theta)f[e(c_{12}\cos\theta)]\cos^{p+\alpha+1}\theta c_{12}^{l+m+p+\alpha+3}\exp\left(-\frac{1}{2}c_{12}^2\right), \end{aligned} \tag{A2}$$

$$\begin{aligned} J_{k,l,m,1,p,\alpha}\left[f(e)\right] &= \frac{(-1)^{p+1}\cdot 2^{-(k+m-2)/2}}{m+2}\left[1-(-1)^m\right]\Gamma\left(\frac{k+m+4}{2}\right) \\ &\quad\times\int_0^\infty dc_{12}\int_0^1 d(\cos\theta)f[e(c_{12}\cos\theta)]\cos^{p+\alpha+2}\theta c_{12}^{l+m+p+\alpha+3}\exp\left(-\frac{1}{2}c_{12}^2\right), \end{aligned} \tag{A3}$$

$$J_{k,l,m,2,p,\alpha}\left[f(e)\right] = \frac{(-1)^p\cdot 2^{-(k+m-1)/2}}{(m+1)(m+3)}\left[1+(-1)^m\right]\Gamma\left(\frac{k+m+5}{2}\right) \times\int_0^\infty dc_{12}\int_0^1 d(\cos\theta) f[e(c_{12}\cos\theta)]\left(1+m\cos^2\theta\right)\cos^{p+\alpha+1}\theta c_{12}^{l+m+p+\alpha+3}\exp\left(-\frac{1}{2}c_{12}^2\right), \tag{A4}$$

respectively. Using these equations, we can calculate μ_2 and μ_4 as

$$\begin{aligned}\mu_2 &= -\frac{1}{2}\int d\boldsymbol{c}_1\int d\boldsymbol{c}_2\int d\hat{\boldsymbol{k}}\Theta(-\boldsymbol{c}_{12}\cdot\hat{\boldsymbol{k}})|\boldsymbol{c}_{12}\cdot\hat{\boldsymbol{k}}|f^{(0)}(\boldsymbol{c}_1)f^{(0)}(\boldsymbol{c}_2)\Delta[c_1^2+c_2^2]\\ &= \frac{1}{4}\int d\boldsymbol{C}\int d\boldsymbol{c}_{12}\int d\hat{\boldsymbol{k}}\left(1-e(c_{12})^2\right)\Theta(-\boldsymbol{c}_{12}\cdot\hat{\boldsymbol{k}})|\boldsymbol{c}_{12}\cdot\hat{\boldsymbol{k}}|(\boldsymbol{c}_{12}\cdot\hat{\boldsymbol{k}})^2\phi(c_1)\phi(c_2)\\ &\quad\times\left\{1+a_2\left[C^4+(\boldsymbol{C}\cdot\boldsymbol{c}_{12})^2+\frac{1}{16}c_{12}^4+\frac{1}{2}C^2c_{12}^2-5C^2-\frac{5}{4}c_{12}^2+\frac{15}{4}\right]\right\}\\ &= \frac{1}{4}\left\{J_{0,0,0,0,2,0}[1-e^2]+a_2\left(J_{4,0,0,0,2,0}[1-e^2]+J_{0,0,2,0,2,0}[1-e^2]+\frac{1}{16}J_{0,4,0,0,2,0}[1-e^2]\right.\right.\\ &\quad\left.\left.+\frac{1}{2}J_{2,2,0,0,2,0}[1-e^2]-5J_{2,0,0,0,2,0}[1-e^2]-\frac{5}{4}J_{0,2,0,0,2,0}[1-e^2]+\frac{15}{4}J_{0,0,0,0,2,0}[1-e^2]\right)\right\}\\ &= \sqrt{2\pi}(S_1+a_2S_2),\end{aligned} \tag{A5}$$

where S_1 and S_2 are, respectively, given by

$$S_1 = \frac{1}{2}\int_0^\infty dc_{12}\int_0^1 d(\cos\theta)\left(1-e(c_{12}\cos\theta)^2\right)\cos^3\theta c_{12}^5\exp\left(-\frac{1}{2}c_{12}^2\right), \tag{A6}$$

$$S_2 = \frac{1}{32}\int_0^\infty dc_{12}\int_0^1 d(\cos\theta)\left(1-e(c_{12}\cos\theta)^2\right)\cos^3\theta c_{12}^5\left(15-10c_{12}^2+c_{12}^4\right)\exp\left(-\frac{1}{2}c_{12}^2\right). \tag{A7}$$

Similarly, we can obtain the expression of μ_4 as

$$\begin{aligned}\mu_4 &= -\frac{1}{2}\int_0 d\boldsymbol{c}_1\int d\boldsymbol{c}_2\int d\hat{\boldsymbol{k}}\Theta(-\boldsymbol{c}_{12}\cdot\hat{\boldsymbol{k}})|\boldsymbol{c}_{12}\cdot\hat{\boldsymbol{k}}|f^{(0)}(\boldsymbol{c}_1)f^{(0)}(\boldsymbol{c}_2)\Delta[c_1^4+c_2^4]\\ &= -\frac{1}{2}\int_0 d\boldsymbol{C}\int d\boldsymbol{c}_{12}\int d\hat{\boldsymbol{k}}\Theta(-\boldsymbol{c}_{12}\cdot\hat{\boldsymbol{k}})|\boldsymbol{c}_{12}\cdot\hat{\boldsymbol{k}}|\phi(c_1)\phi(c_2)\\ &\quad\times\left\{1+a_2\left[C^4+(\boldsymbol{C}\cdot\boldsymbol{c}_{12})^2+\frac{1}{16}c_{12}^4+\frac{1}{2}C^2c_{12}^2-5C^2-\frac{5}{4}c_{12}^2+\frac{15}{4}\right]\right\}\\ &\quad\times\left\{2(1+e)^2\left(\boldsymbol{C}\cdot\hat{\boldsymbol{k}}\right)^2(\boldsymbol{c}_{12}\cdot\hat{\boldsymbol{k}})^2+\frac{1}{8}(1-e^2)^2(\boldsymbol{c}_{12}\cdot\hat{\boldsymbol{k}})^4-\frac{1}{4}(1-e^2)c_{12}^2(\boldsymbol{c}_{12}\cdot\hat{\boldsymbol{k}})^2\right.\\ &\quad\left.-(1-e^2)C^2(\boldsymbol{c}_{12}\cdot\hat{\boldsymbol{k}})^2-4(1+e)(\boldsymbol{C}\cdot\boldsymbol{c}_{12})\left(\boldsymbol{C}\cdot\hat{\boldsymbol{k}}\right)(\boldsymbol{c}_{12}\cdot\hat{\boldsymbol{k}})\right\}\\ &\equiv \sqrt{2\pi}(T_1+a_2T_2),\end{aligned} \tag{A8}$$

where T_1 and T_2 are, respectively, defined by

$$\begin{aligned}T_1 &= \frac{1}{8}\int_0^\infty dc_{12}\int_0^1 d(\cos\theta)\left(1-e(c_{12}\cos\theta)^2\right)\cos^3\theta c_{12}^5\\ &\quad\times\left[10+2c_{12}^2-\left(1-e(c_{12}\cos\theta)^2\right)\cos^2\theta c_{12}^2\right]\exp\left(-\frac{1}{2}c_{12}^2\right),\end{aligned} \tag{A9}$$

$$\begin{aligned}T_2 &= \frac{1}{128}\int_0^\infty dc_{12}\int_0^1 d(\cos\theta)\left(1-e(c_{12}\cos\theta)^2\right)\cos^3\theta c_{12}^5\\ &\quad\times\left[2(-25-7c_{12}^2-5c_{12}^4+c_{12}^6)+\cos^2\theta c_{12}^2(17+10c_{12}^2-c_{12}^4)\right.\\ &\quad\left.+e(c_{12}\cos\theta)^2\cos^2\theta c_{12}^2\left(15-10c_{12}^2+c_{12}^4\right)\right]\exp\left(-\frac{1}{2}c_{12}^2\right)\\ &\quad+\frac{1}{2}\int_0^\infty dc_{12}\int_0^1 d(\cos\theta)\left(1+e(c_{12}\cos\theta)\right)\left(1-\cos^2\theta\right)\cos^3\theta c_{12}^7\exp\left(-\frac{1}{2}c_{12}^2\right).\end{aligned} \tag{A10}$$

APPENDIX B: DISCONTINUOUS LIMIT OF THE MOMENT OF THE DIMENSIONLESS COLLISION INTEGRAL

In this appendix, we derive the expressions of the second and the fourth moments of the collision integral to calculate a_2 in the discontinuous limit ($\beta v^* \to \infty$). In this limit, the velocity dependence of the restitution coefficient (2) reduces to

$$e(v_n) = 1 - (1 - e^*)\Theta(v - v^*). \tag{B1}$$

Inserting this expression into Eqs. (8) and (9), we can obtain following expressions of μ_2 and μ_4:

$$\mu_2^{(\infty)} = \sqrt{2\pi}\left(S_1^{(\infty)} + a_2 S_2^{(\infty)}\right), \tag{B2}$$

$$\mu_4^{(\infty)} = \sqrt{2\pi}\left(T_1^{(\infty)} + a_2 T_2^{(\infty)}\right), \tag{B3}$$

with

$$S_1^{(\infty)} = \left(1 - e^{*2}\right)(1 + x)e^{-x}, \tag{B4}$$

$$S_2^{(\infty)} = \frac{3}{16}\left(1 - e^{*2}\right)\left(1 + x + \frac{x^2}{3}\right)e^{-x}, \tag{B5}$$

$$T_1^{(\infty)} = \left(1 - e^{*2}\right)\left[\frac{9}{2}\left(1 + x + \frac{x^2}{9}\right) + e^{*2}\left(1 + x + \frac{x^2}{2}\right)\right]e^{-x}, \tag{B6}$$

$$T_2^{(\infty)} = \frac{3}{32}\left(1 - e^{*2}\right)\left[69\left(1 + x + \frac{119x^2}{207} + \frac{32x^3}{207} + \frac{4x^4}{207}\right) + 10e^{*2}\left(1 + x + \frac{x^2}{2} + \frac{2x^3}{15} + \frac{2x^4}{15}\right)\right]e^{-x} - 2\left(1 - e^*\right)(1 + x)e^{-x} + 4, \tag{B7}$$

with $x = T^*/(2T)$. It should be noted that the expression of S_1 is equivalent to the previous result[12] because this term comes from the Maxwellian. We can also obtain the expression of $a_2^{(\infty)}$ as

$$a_2^{(\infty)} = \frac{T_1^{(\infty)} - 5S_1^{(\infty)}}{5S_1^{(\infty)} + 5S_2^{(\infty)} - T_2^{(\infty)}} \equiv \frac{N^{(\infty)}}{D^{(\infty)}}, \tag{B8}$$

where $N^{(\infty)}$ and $D^{(\infty)}$ are, respectively, given by

$$N^{(\infty)} = -\frac{1}{2}\left(1 - e^{*2}\right)\left[\left(1 + x - x^2\right) - e^{*2}\left(2 + 2x + x^2\right)\right]e^{-x}, \tag{B9}$$

$$D^{(\infty)} = -\frac{1}{32}\left(1 - e^{*2}\right)\left[\left(17 + 17x + 109x^2 + 32x^3 + 4x^4\right) + e^{*2}\left(30 + 30x + 15x^2 + 4x^3 + 4x^4\right)\right]e^{-x} + 2\left(1 - e^*\right)(1 + x)e^{-x} - 4. \tag{B10}$$

[1] C. D. Stow, "Dust and sand storm electrification," Weather **24**, 134–144 (1969).
[2] H. F. Eden and B. Vonnegut, "Electrical breakdown caused by dust motion in low-pressure atmospheres: Considerations for Mars," Science **180**, 962–963 (1973).
[3] A. A. Mills, "Dust clouds and frictional generation of glow discharges on Mars," Nature **268**, 614 (1977).
[4] J. S. Gilbert, S. J. Lane, R. S. J. Sparks, and T. Koyaguchi, "Charge measurements on particle fallout from a volcanic plume," Nature **349**, 598–600 (1991).
[5] S.-C. Liang, J.-P. Zhang, and L.-S. Fan, "Electrostatic characteristics of hydrated lime powder during transport," Ind. Eng. Chem. Res. **35**, 2748–2755 (1996).
[6] G. Hendrickson, "Electrostatics and gas phase fluidized bed polymerization reactor wall sheeting," Chem. Eng. Sci. **61**, 1041–1064 (2006).
[7] P. K. Haff, "Grain flow as a fluid-mechanical phenomenon," J. Fluid Mech. **134**, 401–430 (1983).
[8] I. Goldhirsch, S. H. Noskowicz, and O. Bar-Lev, "The homogeneous cooling state revisited," Lect. Notes Phys. **624**, 37–63 (2003).
[9] I. Goldhirsch and G. Zanetti, "Clustering instability in dissipative gases," Phys. Rev. Lett. **70**, 1619–1622 (1993).
[10] N. Brilliantov, C. Salueña, T. Schwager, and T. Pöschel, "Transient structures in a granular gas," Phys. Rev. Lett. **93**, 134301 (2004).
[11] T. Scheffler and D. E. Wolf, "Collision rates in charged granular gases," Granular Matter **4**, 103–113 (2002).
[12] T. Pöschel, N. V. Brilliantov, and T. Schwager, "Long-time behavior of granular gases with impact-velocity dependent coefficient of restitution," Phys. A **325**, 274–283 (2003).
[13] N. V. Brilliantov and T. Pöschel, *Kinetic Theory of Granular Gases* (Oxford University Press, New York, 2004).
[14] I. Goldhirsch and T. P. C. van Noije, "Green-Kubo relations for granular fluids," Phys. Rev. E **61**, 3241–3244 (2000).
[15] J. W. Dufty and J. J. Brey, "Green–Kubo expressions for a granular gas," J. Stat. Phys. **109**, 433–448 (2002).
[16] J. J. Brey, J. W. Dufty, C. S. Kim, and A. Santos, "Hydrodynamics for granular flow at low density," Phys. Rev. E **58**, 4638–4653 (1998).
[17] S. E. Esipov and T. Pöschel, "The granular phase diagram," J. Stat. Phys. **86**, 1385–1395 (1997).
[18] A. Goldshtein and M. Shapiro, "Mechanics of collisional motion of granular materials. Part 1. General hydrodynamic equations," J. Fluid Mech. **282**, 75–114 (1995).
[19] N. V. Brilliantov and T. Pöschel, "Velocity distribution in granular gases of viscoelastic particles," Phys. Rev. E **61**, 5573–5587 (2000).
[20] G. A. Bird, *Molecular Gas Dynamics and the Direct Simulation of Gas Flows* (Oxford University Press, New York, 1994).
[21] F. J. Alexander and A. L. Garcia, "The direct simulation Monte Carlo method," Comput. Phys. **11**, 588–593 (1997).
[22] A. J. Garcia, *Numerical Methods for Physics*, 2nd ed. (Prentice Hall, Englewood Cliffs, NJ, 2000).
[23] T. Pöschel and T. Schwager, *Computational Granular Dynamics* (Springer, Berlin, 2005).
[24] K. Nanbu, "Direct simulation scheme derived from the Boltzmann equation. I. Monocomponent gases," J. Phys. Soc. Jpn. **49**, 2042–2049 (1980).
[25] K. Nanbu, "Interrelations between various direct simulation methods for solving the Boltzmann equation," J. Phys. Soc. Jpn. **52**, 3382–3388 (1983).